CDF/PHYS/ELECTROWEAK/GROUP/10642
Version 2.0
April 30, 2012

A Novel Technique to reconstruct the Z mass in WZ/ZZ events with lepton(s), MET and Three Jets.

G. Bellettini, G. Latino, V. Rusu, M. Trovato, G. Velev, C. Vernieri

Abstract

Observing WZ/ZZ production at the Tevatron in a final state with a lepton, missing transverse energy and jets is extremely difficult because of the low signal rate and the huge background. In an attempt to increase the acceptance we study the sample where 3 high energetic jets are reconstructed, where about 1/3 of the process is expected to end. Rather than choosing the two E_T-leading jets to detect a Z signal, we make use of the information carried by all jets.
This study is performed on simulated WZ, ZZ, WW, top events (`PYTHIA`) and W/Z+jets events (`ALPGEN` + `PYTHIA`), with a final state signature of a high-momentum lepton, large $\not\!\!E_T$, and three energetic jets. In WZ/ZZ events the additional jet is produced by the initial or final state radiation. In such a sample the Z mass would normally be defined as the invariant mass of the two leading jets in E_T. We consider how to improve the Z mass resolution by making use of the information carried by the sub-leading jets when 3 large-E_T jets are present.
To qualify the potential of the method we apply our procedure to all diboson events including WW besides WZ, ZZ. We estimate the probability at three standard deviations level to extract an inclusive diboson signal in the 3-jets sample alone (P3σ). After our procedure for building the Z mass is applied, P3σ is about 4 times greater than when building the Z mass "by default" with the two E_T leading jets.
The next step would be to discriminate against the WW contribution by investigating both the samples with two and three clustered jets. Although a consistent improvement in sensitivity over the option of building the Z-mass from J1J2 is observed in the three jet region alone, such an improvement becomes modest when we simultaneously fit in the two and three jet regions. This is due to the fact that the 3 jet sample plays a minor role in the overall sensitivity.

The study presented in this note is mostly MC-based and was performed by assuming an integrated luminosity of about 6.9 fb^{-1}

Contents

1 Motivations

Observing associated WZ production at the Tevatron in the channel $WZ \to \ell\nu q\bar{q}$ is extremely difficult for two main reasons.
The event rate is extremely low. A WZ production cross section of $\sim 3,22$ pb [3] together with a $Z \to hadrons$ branching ratio of $\sim 70\%$ [4] provide about 200 fb in the $WZ \to \ell\nu q\bar{q}$ channel. With a trigger and kinematical selection efficiency of the order of a few %, one expects a small number of events per fb^{-1} of integrated luminosity.
A standard kinematical cut requests exactly two high energy jets (i.e. $E_T > 20$ GeV) in the candidate sample. Simulations show that if a third high energy jet is allowed the signal acceptance is increased by 1/3. Therefore, it would be extremely important to be able to detect the Z signal also in events with more than two high energy jets.
A serious difficulty is that the signal to background ratio is very poor, due primarily to the contribution of associated production of W and incoherent jets. Optimal mass resolution of jet systems is of utmost importance for discriminating this background, since a fit to the invariant mass distribution of the jets associated to the hadronic decay of Z is used to disentangle the diboson signal from the backgrounds.

2 Origin of the Extra Jet

In the case of WZ events, additional jets may be initiated by gluon(s) radiated from the interacting partons (Initial State Radiation, ISR) or from the Z-decay products (Final State Radiation, FSR). Extra-activity produced by spectator partons or by pile-up of events is negligible in our studies.

3 Three jets Region

3.1 Event selection

The study presented in this note is performed in a sample selected as described below. Jet energies are corrected up to L7.

- at least one lepton, "lep1" (TCE,CMUP,CMX), with $E_T(P_T) > 20\ GeV(GeV/c)$
- $\not\!\!E_T > 20\ GeV$
- exclusively three jets with $E_T > 25, 15, 15\ GeV$ and $|\eta| < 2, 2, 3.6$ respectively. No additional jet with $E_T > 10\ GeV$ and $|\eta| < 3.6$ is allowed in the sample.
- metsig[1]>1.8, $M_T^W > 30\ GeV$ when lep1=TCE; $M_T^W > 30\ GeV$ when lep1=CMUP,CMX

Selected sample is dividided in two subsamples depending on the jet flavor. A heavy flavor enriched region ("tag") is isolated from the rest ("notag") by requiring that the two highest-bness jets pass the following cuts

- jet1 bness > 0.75
- jet2 bness > -0.2

Expected rates in the notag and tag samples are reported in Tables 1, 2.
Further details about the selection criteria and how the event yields are estimated can be found in [19]

3.2 Importance of the Three jets Region and Combinatorics Problem

About 33% of diboson events lies in the three jets region, but jets due to initial or final state radiation confuse the choice of the jet system to be attributed to Z decay.
In Fig. 1 the invariant mass built using the two E_T leading jets for WZ MC events in the *two jets region*[2] is compared with the same distribution built in the *three jets region*. In the sample where three jets are found MJ1J2 has a degraded resolution: high mass and low mass tails due to wrong combinations can be observed (Fig. 1).
Choosing the correct jet combination coming from Z for building the Z mass would improve the resolution.

[1] [20]
[2] Events with a third jet with $E_T > 15$ GeV are rejected.

Process	Rate (TCE)	Rate (CMUP,CMX)
Signal	66.2 ± 0.9	69.5 ± 0.9
WW	386.2 ± 3.0	311.1 ± 3.1
$t\bar{t}$	333.0 ± 1.4	288.5 ± 1.1
single-top	68.9 ± 0.4	57.8 ±0.3
Z+jets	350.0 ± 3.2	1167.8 ± 4.5
W+jets	10304.2 ± 29.6	8275 ± 22.8
QCD	1600.4 ± 60.0	353.3 ± 5.4
Total Observed	13109.0 ± 114.5	10522.0 ± 102.6

Table 1: Predicted and observed number of events of the notag sample selected according to the requirements described in Sec. 3.1. W+jets and QCD rates are estimated from fitting the data in either $\not\!\!E_T$(TCE) or M_T^W (CMUP,CMX) ([19]). The expected rates are separated for the triggered lepton type. We also require the invariant mass of the two E_T-leading jets to be within [30,310] GeV/c^2
. By construction the overall expected rates are the same as the observed ones in each region.

Process	Rate (TCE)	Rate (CMUP,CMX)
Signal	3.5 ± 0.2	3.6 ± 0.2
WW	6.2 ± 0.4	4.7 ± 0.3
$t\bar{t}$	146.4 ± 0.9	127.9 ± 0.8
single-top	22.5 ± 0.2	18.7 ±0.2
Z+jets	8.0 ± 0.4	23.6 ± 0.6
W+jets	212.0 ± 3.9	189.9 ± 3.2
QCD	32.5 ± 0.3	5.7 ± 0.0
Total Observed	431.0 ± 20.8	374.0 ± 19.3

Table 2: Predicted and observed number of events of the tag sample selected according to the requirements described in Sec. 3.1. W+jets and QCD rates are estimated from fitting the data in either $\not\!\!E_T$(TCE) or M_T^W (CMUP,CMX) ([19]). The expected rates are separated for the triggered lepton type. We also require the invariant mass of the two E_T-leading jets to be within [30,310] GeV/c^2
. By construction the overall expected rates are the same as the observed ones in each region.

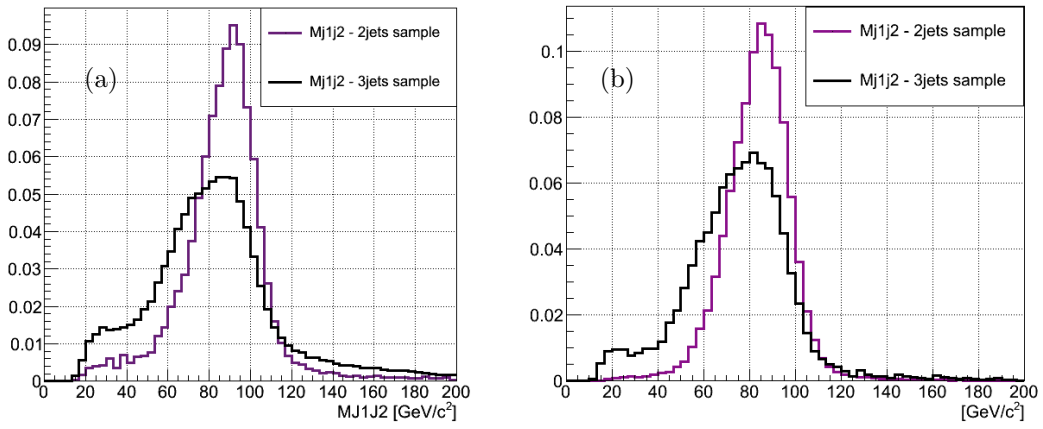

Figure 1: The black distribution is dijet mass built with the two leading jets in the *three jets region*, while the violet one is the invariant mass in the *two jets region*, in *notag* (a) and *tag* (b) sample.

3.3 The importance of knowing the correct jet system

We started from studying the three jets sample in WZ events simulated by PYTHIA [3]. Jets are ordered in decreasing E_T in *notag* sample and in decreasing $b$ness in *tag* sample[4].
We investigate at generator level the origin of the not-matched jet (NMJ) in order to understand the Right Jet Combination (RJC).

3.3.1 Matching jets to quarks

Jets are matched in direction to quarks from Z decay, requiring $\Delta R < 0.4$ between partons from Z and jets. When a number of matches different from 2 is found the event is not considered. In $\sim 33\%$ of cases two or more jets are not matched and are not considered in our studies.
In Fig. 2 the invariant mass distribution of the two E_T-leading jets, is shown in the sample in which we require both jets to be matched to quarks from Z, in the whole sample and in the subsample in which there is no double-match.
The MJ1J2 distribution in the sample rejected for our studies, i.e. the one with no double-match, has the peak shifted to a mass region lower than expected $Z-$mass value. Our guess is that FSR is responsible for the excluded events (a hard gluon radiation compromises the match to the initial parton).

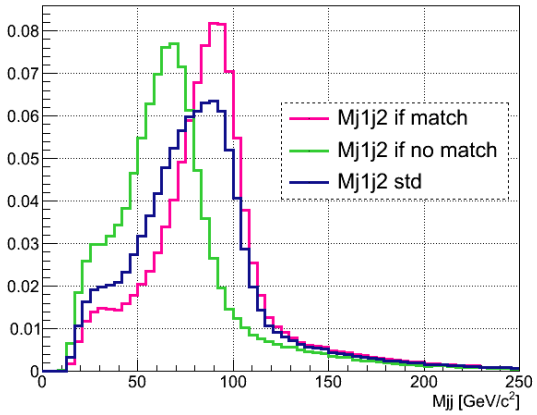

Figure 2: Invariant mass distribution in the 3 jets region built with the two E_T-leading jets in the whole *notag* sample, in the subsample in which the double-match requirement is satisfied and in the complementary one.

In the double-match sample we investigate the origin of the NMJ. We identify all the partons within a $R = 0.4$ cone about the NMJ direction and we separate two cases:

1. partons are radiated from the interacting partons, i.e. ISR
2. partons are radiated from the $q\bar{q}$ pair from Z, i.e. FSR

The sums of the energies of the aforementioned partons are computed. We state that a jet comes from ISR if the energy from FSR is 0 and viceversa.
In 6% of the events we found that NMJ have both ISR and FSR energies different than 0. Those events are rejected. In about 10% of the events we can't trace back the origin of the parton in the NMJ cone. Also those events are discarded.

3.3.2 Matching jets to stable hadrons

Requiring 2 jets matched to $q/\bar{q}$ from Z selects a limited event sample (66%). However we are unable to match the third jet to either ISR/FSR gluons in the $\sim$15% of these events. So, we are able to assign the proper RJC only in the 56% of events and NNs cannot be trained on the excluded events.

[3] The *sam* dataset used are: `ht0swz`, `it0swz`, `jhhs10`, `jhhs11`, `jhhs1a`, `wz0s1a`, `wzhs1b`
[4] J1, J2 would be the two with highest $b$ness value, J3 the one with highest E_T among the others.

We expect that improving the matching algorithm will improve our NNs efficiency, since it allow us to train the NNs with a set of events with a kinematics as close as possible to the signal in data.
In order to to rescue these events, we decide to implement a different matching algorithm. This algorithm searches for hadrons rather than quarks in the jet cone and traces back via the strings [5] the origin of the hadrons. If the hadrons originated from a primary beam parton, we state that the hadrons come from ISR, otherwise if the hadron origin is the q or $\bar{q}$ from Z, we state that the hadrons comes from FSR. By doing so, we are able to understand the origin of the jet in $\sim 99\%$. Sometimes we found both ISR and FSR hadrons in the jet cone. We decide to label the jet as an ISR/FSR jet if the hadron energy from ISR/FSR is more than FSR/ISR energy.

The rate of matching is not 100% because we have few events in which one jet is not matched to hadrons. We guess matching could fail because there is no magnetic field curving the hadrons. Matching to the "OBSP particle" could recover these cases.

By construction we expect at least two jets from FSR (i.e. jets originated by $q/\bar{q}$ from Z). But, in 2,7% of the cases our algorithm fails and we are not able to find them. We investigate these events and we see that it is due to the not reconstruction of one of the two Z-jets. The reason could be the calorimeter cracks in $\eta \sim |1|$ region, or the different calorimeter granularity for $\eta \sim |2|$ region, see Fig. 3. We consider negligible this effect, also because for these few events the matching to quarks algorithm fails too.

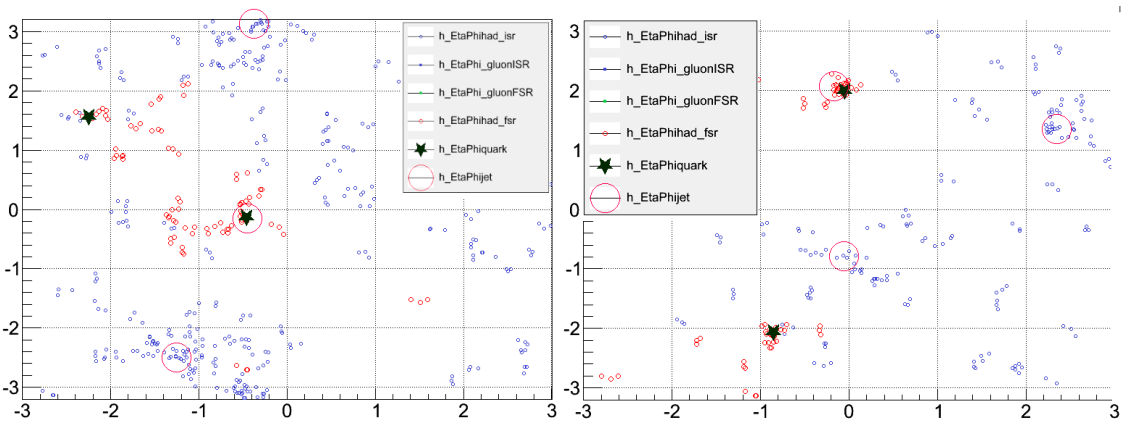

Figure 3: $\eta - \phi$ distribution of stable hadrons which comes from ISR and FSR, quarks and jets for two particular events in which only one jet from FSR is identified.

3.4 Notag

Once the origin of each jet is well understood we know which is the RJC event by event. In terms of the frequency of RJC the notag sample is composed as follows:

1. NMJ = J3 is from ISR $\mapsto$ RJC = J1J2 - 33.5% of events
2. NMJ = J2 is from ISR $\mapsto$ RJC = J1J3 - 20.4% of events
3. NMJ = J1 is from ISR $\mapsto$ RJC = J2J3 - 10% of events
4. NMJ is from FSR $\mapsto$ RJC = J1J2J3 - 33.3% of events

The best resolution we can get in this sample is shown in Fig. 4-5, where we compare the invariant mass built using the proper RJC for each event with the distribution built with the two E_T leading jets (Fig. 4) and with the dijet mass in the *two jets region* (Fig. 5). The low and high mass tails affecting the MJ1J2 distribution are drastically reduced by choosing the correct combination. Moreover, choosing the correct combination would allow us to have in the three jets region the same resolution as in the two jets region.

As a test of the method we compare the M_{RJC} distributions using matching to hadrons rather than matching to partons. In the double sample with two jets matched to quarks from Z (56%) we obtain the same results, see Fig. 6 and also Appendix A for more details.

[5] In `PYTHIA` the intermediate objects between partons and hadrons are called "strings".

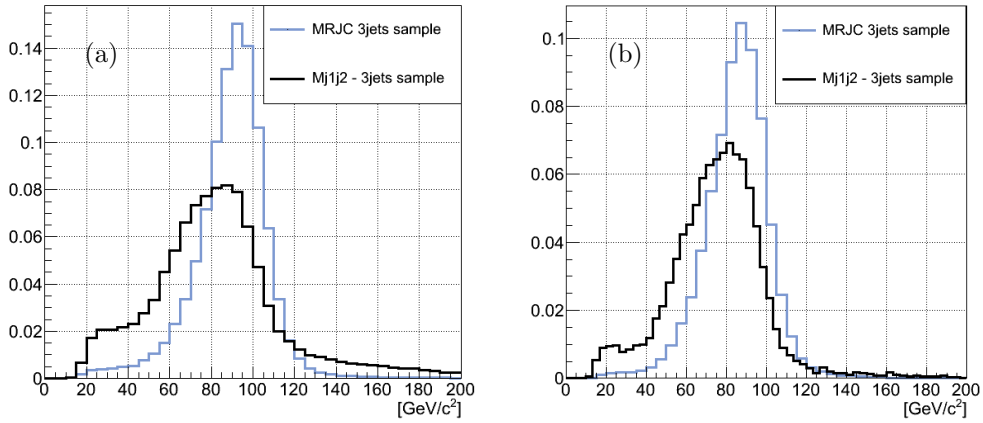

Figure 4: The blue invariant mass is built using the two 'Z-jets' when the 3^{rd} jet is from ISR and combining the 3 jets if FSR. The black distribution is dijet mass built with the two leading jets, in *notag* (a) and *tag* (b) sample.

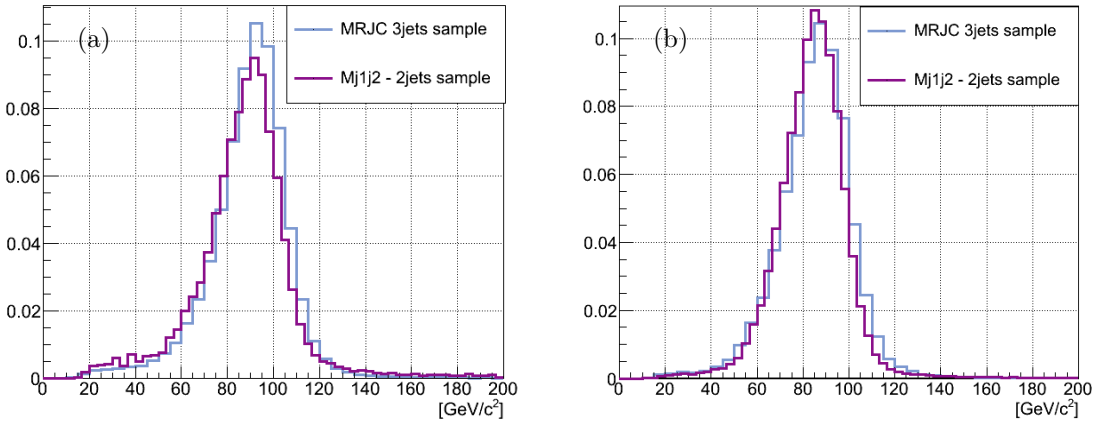

Figure 5: The blue invariant mass is the M_{RJC} distribution, built using the two 'Z-jets' when the 3^{rd} jet is from ISR and combining the 3 jets if FSR; the violet distribution is the invariant mass in the tight dijet sample, in *notag* (a) and *tag* (b) sample.

3.5 Tag

In terms of the frequency of RJC the tag sample is composed as follows:

1. NMJ = J3 is from ISR $\mapsto$ RJC = J1J2 - 53.4% of events
2. NMJ = J2 is from ISR $\mapsto$ RJC = J1J3 - 9.5% of events
3. NMJ = J1 is from ISR $\mapsto$ RJC = J2J3 - 4.1% of events
4. NMJ is from FSR $\mapsto$ RJC = J1J2J3 - 31.2% of events

Notice that in *tag* sample MJ1J2 is the RJC in the 53.4% of cases, since jets are ordered in *b*ness and we require the two *b*ness leading jets to satisfy some criteria. The greater contribution of MJ1J2 in the whole sample is the reason why in the *tag* sample the resolution is already good for the distribution built with the two jets with highest *b*ness. As a consequence, we expect that there is less to improve in this sample. The best resolution we can get in this sample is shown in Fig. 4-5, where we compare the invariant mass built using the proper RJC for each event with the distribution built with the two E_T leading jets (Fig. 4) and with the dijet mass in the *two jets region* (Fig. 5). The low and high mass tails affecting the MJ1J2

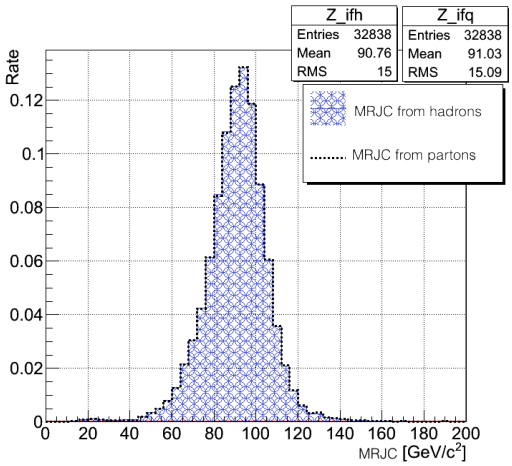

Figure 6: In the fully matched sample (∼56%) we compare the M_{RJC} distributions built using matching to hadrons rather than matching to partons.

distribution are drastically reduced by choosing the correct combination.

4 Adopted strategy: Neural Networks

Four different Neural Networks (NNs) have been trained, using MLP method [5], in MC signal events to isolate each of the above cases: NN_{12}, NN_{13}, NN_{23} and NN_{123}. These NNs combine kinematical information and some tools developed by CDF Collaboration for discriminating gluon-like and b-like jets from light-flavored jets [11, 18]. Inputs to NNs are:

1. Kinematical variables:
   $d\eta_{j_ij_k}$, $dR_{j_ij_k}$, $dR_{j_i\ell}$, $dR_{j_kj_l,j_p}$, $dR_{j_1j_2j_3,j_k}$[6]
2. Variables related to the jet systems:
   - $m_{j_ij_k}/m_{j_1j_2j_3}$
   - $\gamma_{j_ij_k} = (E_{j_i} + E_{j_k})/m_{j_ij_k}$
   - $\gamma_{jjj} = (E_{j_1} + E_{j_2} + E_{j_3})/m_{j_1j_2j_3}$
   - 'pt-imbalance' $= P_{TJ1} + P_{TJ2} - P_{T\ell}$- MET
   - $\eta(j_i + j_k)/\eta(j_p)$, $p_T(j_i + j_k)/p_T(j_p)$
3. b/light quark discriminant, quark/gluon discriminant.

Based on the response of the four NNs, we determine the most likely jet combination for building the Z mass for each event. The method allows to use a different combination from J1J2 in about 66.5% (46.6%) of cases in the notag (tag) sample.

4.1 The "Novel technique" in notag sample

Here we present only the criteria and the obtained results and the details relates to one NN.
A detailed description of the other NNs used in the *notag* sample is in Appendix B.

4.2 Exploring MJ1J2: NN_{12}

In order to isolate events when RJC = J1J2 we analyze differences of some variables in two subsamples:

- RJC = J1J2
- Other jet combinations (RJC = J1J3, J2J3, J1J2J3, UNKNOWN) which we name "OJC"

[6] i, k, p = 1; 2; 3. ℓ = highest E_T lepton

Below is the list of the variables used (see also Fig. 8):

1. $m_{jj'}/m_{j_1j_2j_3}$[7]
2. $\gamma_{jj'} = (E_j + E_{j'})/m_{jj'}$
3. d$\eta_{jj'}$
4. $dR_{jj'}$
5. $dR_{j_1j_2,j_3}$, dR between the third jet and vectorial sum of the two leading jets.
6. $dR_{j_1j_2j_3,j_3}$, dR between the third jet and vectorial sum of the three jets.
7. Z_{p_t}
8. "pt-imbalance" (Sec. 4)
9. Ht
10. Quark Gluon Discriminator for J2, J3 used for discriminating a quark from a gluon jet [18].

In order to avoid background (W+jets, $t\bar{t}$, etc...) being sculpted later, the input variables are weighted. Weights applied are calculated such that the MJ1J2 distribution in the OJC sample become approximately the same of the one in the RJC = J1J2 sample. By doing this we will decorrelate the NN_{12} output from the numerical value of MJ1J2 and make it sensitive only to the difference in kinematical distributions of the involved variables. In Fig. 7 the weights used and MJ1J2 distributions before and after normalization in both subsamples are shown.

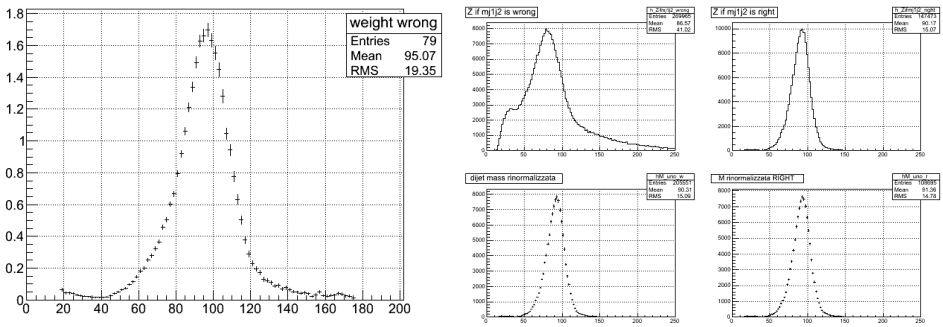

Figure 7: MJ1J2 distribution in the two subsamples before and after normalization (Right). Weights used for normalizing (Left). Above 110 GeV/c^2 and below 80 GeV/c^2 weights are lower than 1 in order to reduce the tails.

4.2.1 Output

The variables described above are weighted accordingly and are used for training a Neural Network, employing the MLP method.
The NN_{12} response is shown in Fig. 9.

4.2.2 Criteria for notag sample

For combining the information provided by the outputs of the four NNs, a criterion for building the invariant mass has been developed. We started with a requirement on NN_{12} and so we select the ∼33.5% of the sample where MJ1J2 is chosen for reconstructing the Z. Next we apply a requirement on NN_{123}, in order to select the subsample where MJ1J2J3 would be used. After we apply a cut on the NN_{13} and NN_{23} outputs. The values for the cuts for each NNs have been chosen in order to select for each of the 4 possible combinations a number of events equal to the expected frequency of the RJC in the selected sample (see sec. 3.4)[8]. We are working to optimize the NN cuts against the sensitivity of the WZ/ZZ cross section measurement.

[7] jj' refers to the three possible combinations: J1J2, J1J3 and J2J3.
[8] with a perfect NN optimization power we would select all the RJC by doing so

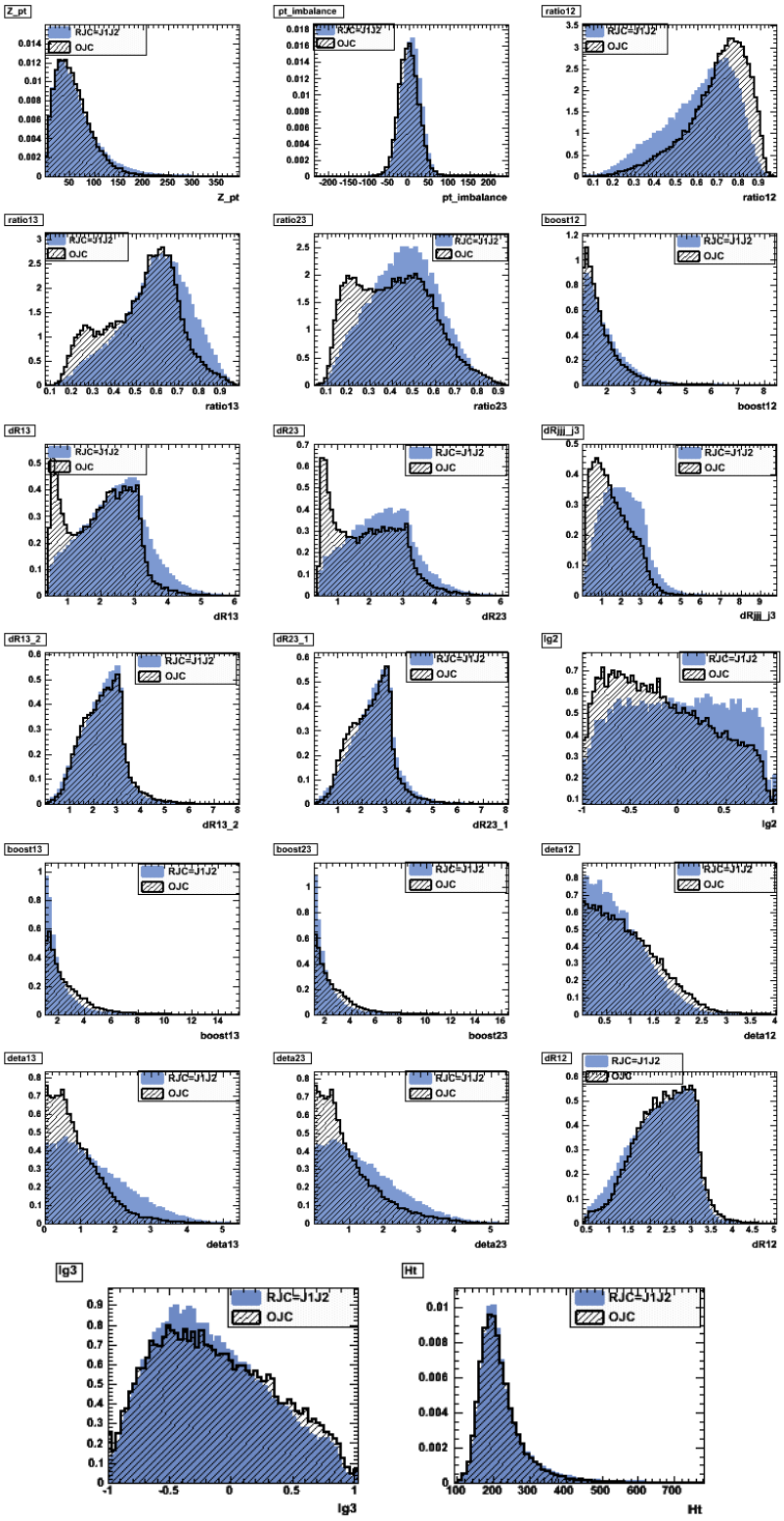

Figure 8: NN_{12} input variables after weighting.

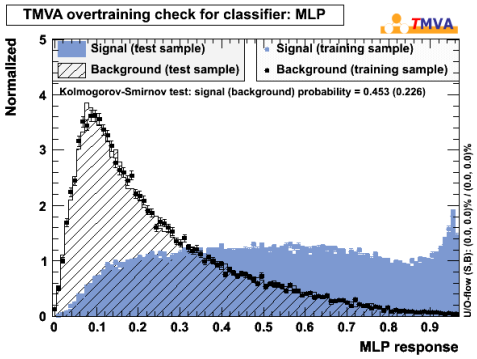

Figure 9: NN_{12} MLP response.

We apply these cuts sequentially since we notice that NN's outputs are decoupled, see Appendix D. The above criterion (see Table 3) allows us to build a MJJ_{COMB} to be used in the *three jets region*, which is shown in Fig. 10 compared with MJ1J2 distribution in the *two jets region*. It is seen that an improvement in resolution is obtained.

NN	MJJ_{COMB}
$NN_{12} > 0.5$	MJ1J2
$NN_{123} > 0.3$	MJ1J2J3
$NN_{13} > 0.55$	MJ1J3
$NN_{23} > 0.55$	MJ2J3

Table 3: Criteria used for building MJJ_{COMB} in notag sample.

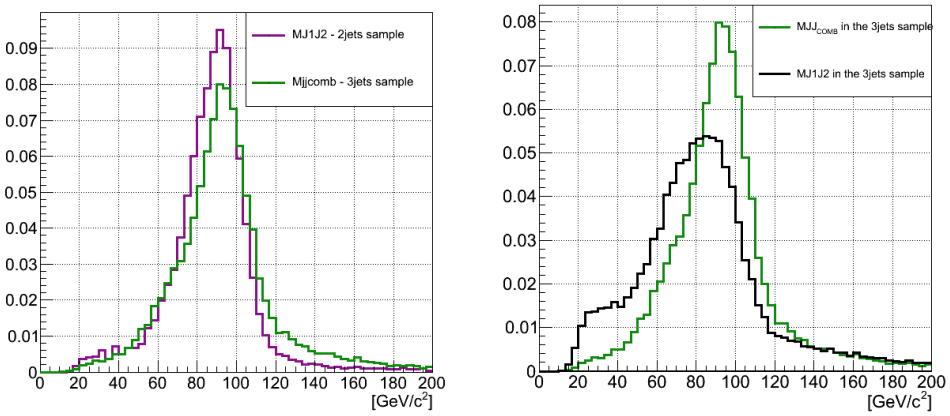

Figure 10: Notag Sample. MJ1J2 in the *two jets region* (violet) and MJ1J2 in the *three jets region* (black) are compared with MJJ_{COMB} in the *three jets region*.

In order to understand the impact of this method on the sensitivity of the measurement we apply the method also to the major sources of background (W+jets, Z+jets, $t\bar{t}$ and single top) and compare the result to WZ events. In Fig. 11 MJ1J2 and MJJ_{COMB} distributions are shown in signal and background events. The signal is multiplied by 80 in order to facilitate a visual comparison. In Table 4 the acceptance, the *purity p*

defined in 1 and the σ over μ ratio[9] are given.

$$Acc = \frac{Evt^{sel}}{Evt^{tot}} \quad p = \frac{MJJ^{RIGHT}}{Evt^{sel}} \tag{1}$$

where Evt^{sel} is the number of selected events while MJJ^{RIGHT} is the number of the selected events in which we choose the correct RJC.

	std	if **criteria**
Acc	100%	90%
p	35%	65%
σ/μ	0.25	0.13

Table 4: Performance of MJJ_{COMB} in the *notag* sample

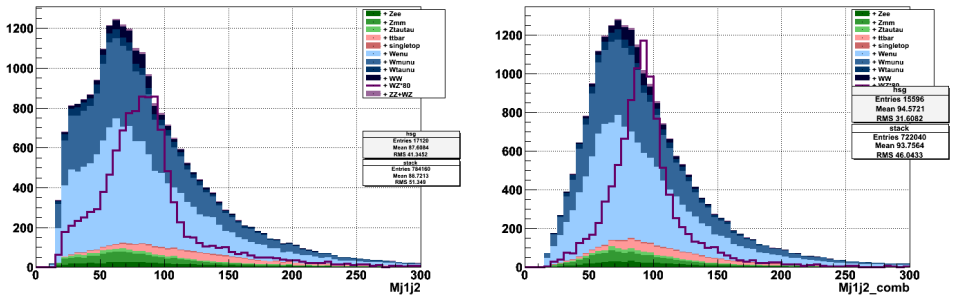

Figure 11: Notag Sample. Simulation of signal+background. Left, MJ1J2. Right, MJJ_{COMB} built with the criteria described in the text. An integrated luminosity of about 6.9 fb^{-1} is assumed when weighting MC events

We note that as a consequence of the above mentioned decorrelation procedure, the invariant mass distribution in the background events get slightly sculpted. In Fig. 12 is shown how change the W+jets contribute using MJJ_{COMB} instead of MJ1J2.

4.3 A comment on the matching algorithm

In order to understand how matching to hadrons helps NNs training we compare in Fig. 13 two MJJ_{COMB} distributions, both built in the sample in which jets to parton matching fails. The green distribution is what

[9] σ and μ are estimated by a Gaussian fit in the mass window [70,110] GeV/c^2, see also Appendix E.1 for more details.

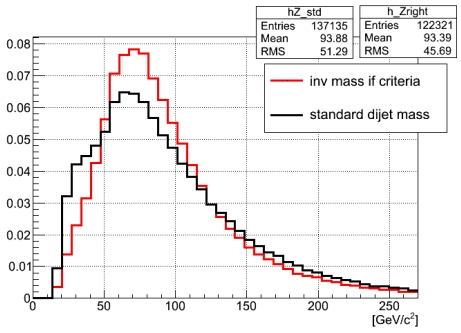

Figure 12: Notag Sample. MJJ_{COMB} is compared to MJ1J2 for W+jets events.

NN	MJJ_{COMB}
$NN_{12} > 0.4$	MJ1J2
$NN_{123} > 0.3$	MJ1J2J3
$NN_{13} > 0.6$	MJ1J3
$NN_{23} > 0.6$	MJ2J3

Table 5: Criteria used for building MJJ_{COMB} in the *tag* sample.

we obtained when we use almost the whole sample for training our NNs. The red distributions instead is built with the information of the NNs trained only with events in which jets are matched to partons.
It can be noticed that now the training, which makes use of almost the whole sample, improves MJJ_{COMB} resolution also for the events to which we were blind with the previous matching algorithm.

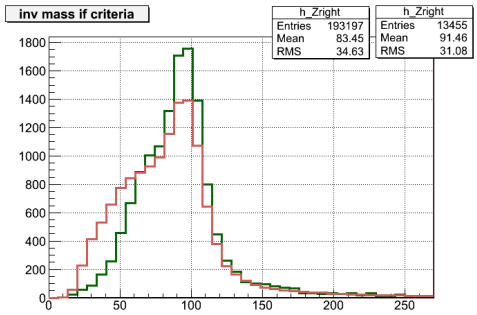

Figure 13: MJJ_{COMB} distributions in the sample in which jets are not matched to partons built using two different sets of NNs. One set is trained in the sample in which jets are matched to hadrons (green), the other (red) trained only with events in which jets are matched to partons.

4.4 The "Novel technique" in tag sample

In the tag sample we used a very similar technique. Differences from the criteria developed in the *notag* sample are mainly in the variables used for training each NN.
Since we expect two b-jets in this sample we also use $b$ness information in our NNs. A detailed description of the NNs used in the tag sample is in Appendix C. Notice in order to obtain enough statistics for NN_{13} and NN_{23} training, we allow events with $b$ness>0.5 as regards the first jet and no $b$ness requirement on the second jet.
Here we present only the criteria and the obtained results.

4.4.1 Criteria for tag sample

The developed criteria (see Table 5) allow building a MJJ_{COMB} for the *three jets region*, as appropriate for the *tag* sample. The obtained mass distribution is compared with MJ1J2 in the *two jets region* in Fig. 14. An improvement in resolution is obtained, although in this sample the resolution of MJ1J2 is already good.

In order to understand the impact of this method on the sensitivity of the measurement we build MJJ_{COMB} in the main sources of background (W+jets, Z+jets, $t\bar{t}$ and single top) and compare it to WZ events. In Fig. 15 MJ1J2 and MJJ_{COMB} distributions are shown in signal and background events. The signal is multiplied by 40 in order to facilitate a visual comparison.
We note that as a consequence of the decorrelation procedure, the invariant mass distribution in the background events doesn't get sculpted under the signal.

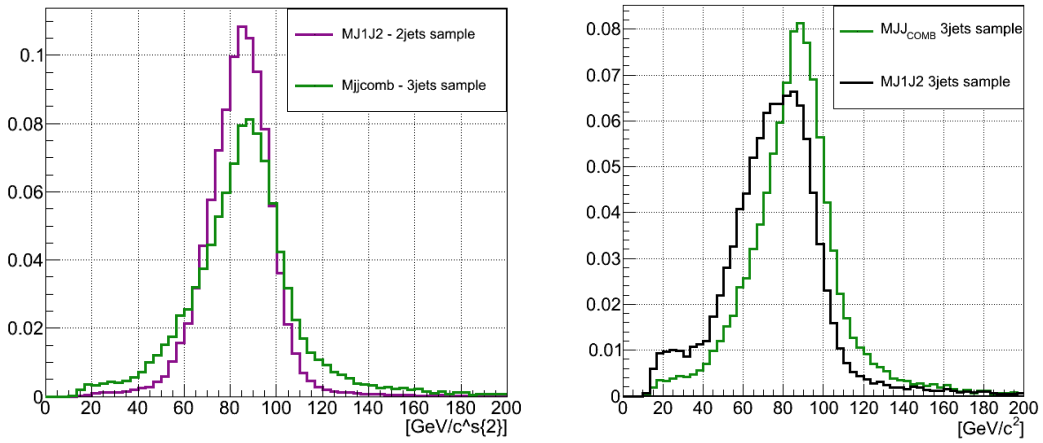

Figure 14: Tag sample. MJ1J2 in the *two jets region* (violet, Left) and in the *three jets region* (black, Right) are compared with MJJ_{COMB} in the *three jets region*.

	std	if **criteria**
Acc	100%	92%
p	53%	72%
σ/μ	0.22%	0.14%

Table 6: Performance of MJJ_{COMB} in the *tag* sample: acceptance, purity and resolution parameters (see Appendix E.1).

5 Modeling

Once the background levels are predicted, we want to investigate the agreement between data and MC of various kinematic distributions. A number of distributions important for the study presented in this note can be found in [19] [10].

[10] In [19] kinematical distributions in MC are compared to data samples of about 8.9 $fb^{-}1$ integrated luminosity. Although the method presented here was derived by assuming a lower integrated luminosity, we don't expect big differences from the change in luminosity since this method is mostly MC-based.

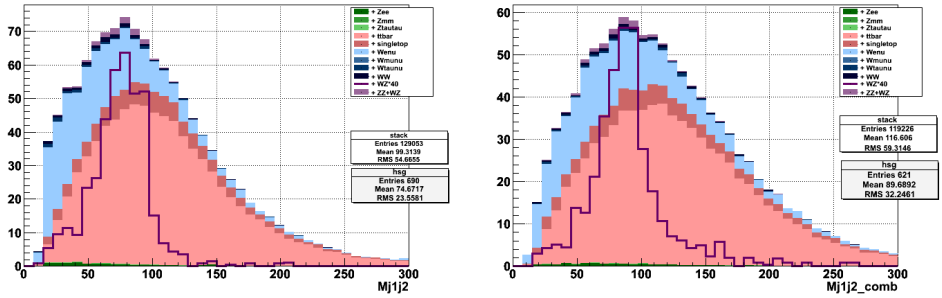

Figure 15: Simulation of signal+background. Left, MJ1J2. Right, MJJ_{COMB} built with the criteria described in the text.

6 Signal Extraction

Our final goal is to extract the signal from the background by fitting the invariant mass distribution in data events. Fits to data (or pseudo-data) are performed using the `mclimit_csm.C` code [14]. Histograms for background and signal are inputed, as well as various systematics as rate and/or shape uncertainties.
We adopt two different fit methods in the *three jets* region:

1. we treat $WW/WZ/ZZ$ as our signal and we fit in the *pretag* region[11]
2. we treat WZ/ZZ as our signal and we fit simultaneously in the tag and notag samples.

The first method is just a check of our technique. Since WW/WZ signal has been observed in CDF [16, 17], it would be an useful test to understand if only the 3-jets sample $WW/WZ/ZZ$[12] signal could be extract. The second method is to extract WZ/ZZ signal. We decide to treat separately *notag* and *tag* regions and then combine the results of both channels in order to reach a greater sensitivity.
The *templates* used are :

- W+jets, whose normalization is allowed to float in the fit unconstrained in the fit independently in the two different channels.
- $t\bar{t}$, single top and Z+jets Gaussian-constrained to the theoretical/measured cross section with uncertainties of 6%.
- QCD data driven estimate, Gaussian-constrained with a systematic uncertainty of 50% in the no-tag channel and its statistical uncertainty in the two-tag channel.
- When treated as a source of background, WW scaled to the NLO cross section, Gaussian-constrained with an uncertainty of 6%.
- WZ/ZZ signal, with normalization allowed to float unconstrained in the fit, but unlike the W+jets background, with rates constrained to the expected relative ratio in the two channels.

Futher details can be found in [19].

6.1 Systematic uncertaintiess

Since this analysis relies so heavily on MC simulation, a large number of systematic uncertainties must be considered to make sure that the data and MC are consistent. Two classes of systematics are considered, those affecting the signal extraction and the additional systematics affecting the acceptance and therefore the signal cross-section.
Table 7 shows the summary of the systematic uncertainties considered in the analysis. We estimate the systematics on the signal extraction by generating pseudo-experiments (PE) using two additional models, corresponding to upward or downward fluctuations of the nuisance parameter for each systematic source. The pseudo-experiments are then fitted using the templates of the main fit on data. For each PE nuisance parameters are varied to get the best agreement between pseudo-data and fitted model. The difference between the central value of the fit on data and the mean of the estimator of the signal content on the two corresponding pseudo-experiments is taken as systematic uncertainty on the corresponding source. For the signal extraction we consider the following sources of systematic uncertainty:

Jet Energy Scale (JES). The corrections used to set the JES are described in sec. **??**. The effect of the JES uncertainty on the measurement is estimated by varying the energy of all jets in MC samples by $\pm 1\sigma$. This procedure is applied at the same time to all the MC based processes. The evaluated systematic is given in Table 7.

b-tagger efficiency/mistag rate. Rather than applying scale factors to the tagging efficiency and mistag rate in order to make simulations to agree with data, we locate the cut in the MC computed efficiency parameter that matches the measured efficiency and mistag rates in the data. In the same manner, we determine the cuts on *b*ness in the MC that match the $\pm 1\sigma$ uncertainty values in the mistag rate and efficiency [11].

Renormalization and Factorization Scales in the W+jets MC (Q^2): the `ALPGEN` event generator used for W+jets events requires renormalization and factorization scales, Q^2, to be set.

[11] No requirement on jet *b*ness: jets of all flavors are accepted.
[12] we expect ZZ contribution to be negligible due to the requirement on $\not\!\!E_T$

Acceptance		**Signal**	**EWK**	**W+jets**	**QCD**	**WW**
JER		0.7%	0.7%	0.7%	no	0.7%
lumi		6%	6%	6%	no	6%
ISR/FSR		2.5%	2.5%	2.5%	no	2.5%
PDF		2%	2%	2%	no	2%
trigger		2.2%	2.2%	2.2%	no	2.2%
Systematic	**channel**	**Signal**	**EWK**	**W+jets**	**QCD**	**WW**
JES shape/rate	notag	yes/$\pm^{1\%}_{18\%}$	yes/$\pm^{3\%}_{13\%}$	yes	no	yes/$\pm^{2\%}_{17\%}$
	tag	yes/$\pm^{9\%}_{16\%}$	yes/$\pm^{13\%}_{18\%}$	yes	no	yes/$\pm^{10\%}_{17\%}$
$b$ness cuts rate	notag	$\mp^{11\%}_{12\%}$	$\mp^{12\%}_{13\%}$	$\pm^{17\%}_{19\%}$	no	$\mp^{6\%}_{18\%}$
	tag	$\pm^{0.7\%}_{0.7\%}$	$\pm^{2\%}_{2\%}$	$\pm^{0.3\%}_{0.3\%}$	no	$\pm^{0.0\%}_{0.3\%}$
Q^2	tag	no	no	yes	no	no
	notag	no	no	yes	no	no

Table 7: Summary of the cuts defining the candidate events samples.

This parameter is doubled and halved to create two samples which are used to determine the shape uncertainty on the W+jets template[13].

In the cross section estimation, we assumed that the luminosity, the lepton trigger efficiency and the MC acceptance were exact. All of these assumptions are later considered as sources of systematics that contribute to the uncertainty of the cross section measurement, in addition to the signal fraction extraction systematics.

Jet Energy Resolution (JER): the modeling of the jet energy resolution (JER) can be a source of systematic uncertainty. It can affect the signal acceptance: if the dijet resonance is wider, more signal events may fall below the jet E_T thresholds or outside the dijet mass window used in the fit. The uncertainty in the jet energy resolution is found to vary as $\Delta(\sigma/p_T)=(0.03\pm1.7)/p_T$ [GeV/c] [12]. Smearing the dijet mass due to energy resolution results in a 0.7% uncertainty in the measured cross section.

ISR/FSR: this systematics affects the acceptance of the MC events. We determine a 2.5% systematic uncertainty due to more/less ISR and FSR.

PDF. We determine the change in the signal acceptance due to the PDF uncertainty to be 2% [13].

Luminosity and trigger efficiency. A 6% uncertainty on the cross section is assigned due to the uncertainty on the luminosity, as determined by the CDF luminosity counters. Uncertainties due to trigger efficiencies are calculated by varying the trigger scale factors[14] within their uncertainties and then applying the shifted scale factors in MC weight. A variation of 2.2% in the number of the expected events is found.

6.2 Sensitivity and Optimization

The `mclimit_csm.C` code provides a means of obtaining an estimate for the probability of a 2σ and 3σ measurement by generating pseudo-experiments and constructing $\Delta\chi^2$ distributions for test and null hypotheses. To obtain acceptable accuracy, we generate about 100,000 pseudo-experiments.

6.3 WZ/ZZ/WW pretag in the 3-jets region

We estimate the probability at two and three standard deviations level to extract an inclusive diboson signal in the 3-jets sample alone (P2σ, P3σ). Systematic uncertainties are not yet included for generating PEs and

[13]Since the theoretical cross section of W+jets is only known to the lowest order in QCD and suffers from large uncertainties, its normalization is derived from data

[14]Trigger scale factors are chosen run-by-run and during data-taking, and are used to weight MC events according to the corresponding trigger efficiency.

for the fits of the pseudo-data. After our procedure for building the Z mass is applied, P3σ is about 4 times greater than when building the Z mass "by default" with the two E_T leading jets, see Table 8.
In Fig. 18 the $\Delta\chi^2$ distributions are shown for MJ1J2 and MJJ$_{COMB}$. The vertical lines show the value of $\Delta\chi^2_{2\sigma}$ ($\Delta\chi^2_{3\sigma}$) such that the probability to have $\Delta\chi^2 < \Delta\chi^2_{2\sigma}$ ($\Delta\chi^2_{3\sigma}$) is 2.3% (0.13%).

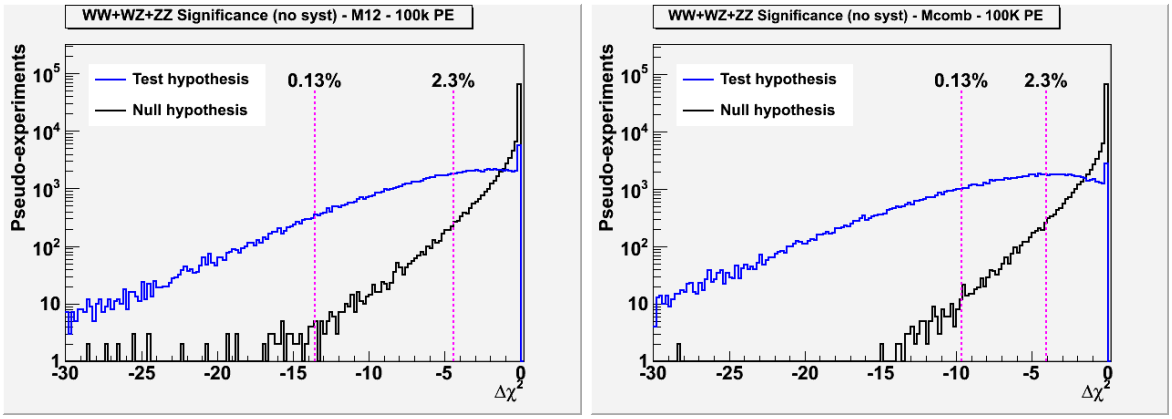

Figure 16: The $\Delta\chi^2$ distributions for null and test hypotheses for the fit to the $WZ/ZZ/WW$ signal, using MJ1J2 (left) and MJJ$_{COMB}$ (right) as the invariant mass in the 3-jets region.

6.4 WZ/ZZ combined double tag+notag

We estimate the expected p-value to extract the WZ/ZZ signal in the 3-jets sample combining the information of the *notag* and *tag* channels. This time the systematic uncertainties described in 6.1 have been included in the fit. The results are shown in Table 8.

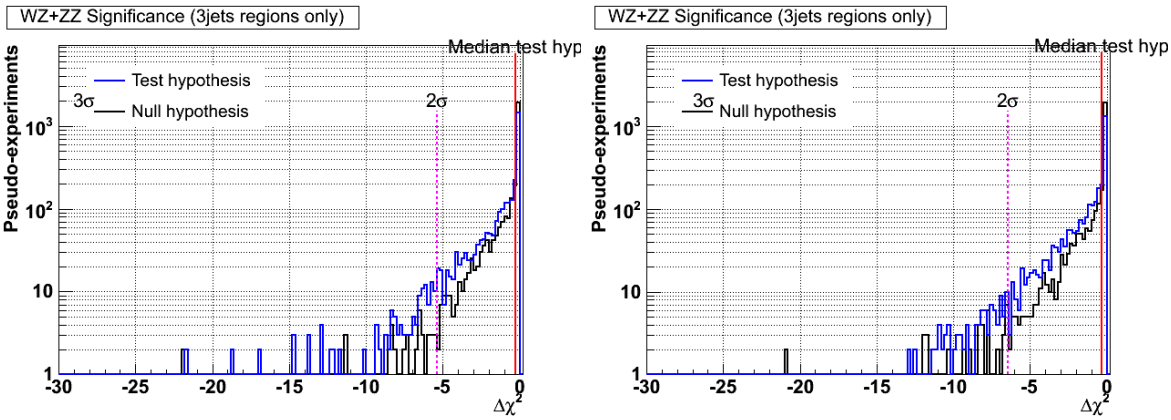

Figure 17: The $\Delta\chi^2$ distributions for null and test hypotheses for the fit to the WZ/ZZ signal, using MJ1J2 (left) and MJJ$_{COMB}$ (right) as the invariant mass in the 3-jets *notag* and *tag* regions.

After applying our technique to build Z mass in the three jets region, the sensitivity increases by about 30%.

7 Concluding Comments

To qualify the potential of the method we have studied an experimental data sample accepting events with a leptonically decaying W and 3 large transverse momentum jets, as in the studies of the simulated WZ

Fit Method	$P_{2\sigma}$	$P_{3\sigma}$
Fit signal $WZ/ZZ/WW$ (pretag)		
- MJ1J2	51.2%	6.4%
- MJJ_{COMB}	66.7%	25.9%
	p-value	
Fit signal WZ/ZZ (notag+tag)		
- MJ1J2	0.35 σ	
- MJJ_{COMB}	0.45 σ	

Table 8: Sensitivity of the fits considering only the 3 jets region.

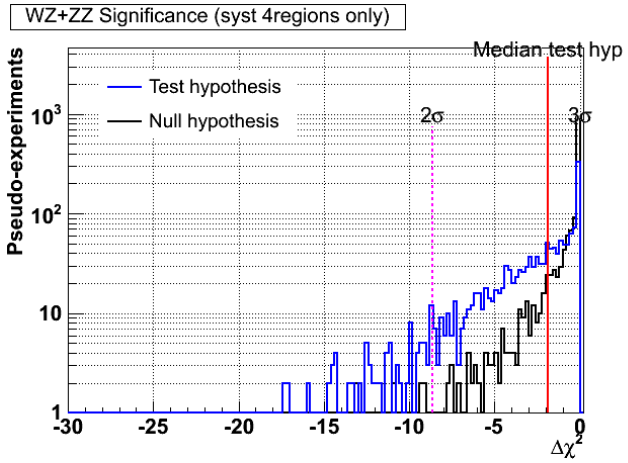

Figure 18: The $\Delta\chi^2$ distributions for null and test hypotheses for the fit to the WZ/ZZ considering both *notag* and *tag* sample combining the 2-jets and 3-jets samples.

sample. The selection cuts accept jets of all flavors (*pretag* sample), and all diboson events including WW besides WZ, ZZ may pass the cuts. We estimate the probability at three standard deviations level to extract an inclusive diboson signal in the 3-jets sample alone (P3σ). After our procedure for building the Z mass is applied, P3σ is about 4 times greater than when building the Z mass "by default" with the two E_T leading jets. Even if the systematic errors were not yet accounted for in this estimate, this appears as a significant progress.

However, in order to discriminate against the WW contribution we apply our technique considering WZ/ZZ as the signal. By investigating the 3-jets *notag* and *tag* regions the sensitivity considerably increases, although only a modest improvement is observed when combining the 3 jet region with the more sensitive two jet region. Still, our technique allows including the three jets sample in the WZ/ZZ analyses in order to increase the acceptance and the sensitivity in the search for the hadronically decaying Z-boson.

References

[1] M. L. Mangano et al *J. High Energy Phys.* **07** (2001) 001

[2] T. Sjöstrand et al *Computer Phys. Commun.* **135** (2001) 238

[3] J. M. Campbell and R. K. Ellis *Update on Vector Boson Pair Production at Hadron Colliders* Phys. Rev. D **65** (2002) 113007.

[4] K. Nakamura et al. (Particle Data Group) J. Phys. G **37** (2010) 075021.

[5] A. Hoecker, P. Speckmayer, J. Stelzer, J. Therhaag, E. von Toerne, and H. Voss *TMVA - Toolkit for Multivariate Data Analysis* (2007) arXiv:physics/0703039

[6] J. Adelman et al. *Method II for you* CDF Note **9185** (2008)

[7] Tom Junk et al. *Combination of CDF's Searches for the Standard Model Higgs boson with up to 8.2 fb^{-1} of Data.* CDF Note **10609** (2011)

[8] T. Aaltonen et al (CDF Collaboration) *Measurement of Inclusive Jet Cross Sections in $Z/\gamma^*(\rightarrow e^+e^-)$+ jets Production in $p\bar{p}$ Collisions at $\sqrt{s}$1.96 TeV* Phys. Rev. Lett. **100** (2008) 102001

[9] Frankiln et al. *Calibration of Heavy-Flavor Production in QCD Data* CDF Note **8768** 2007

[10] Frankiln et al. *Heavy-Flavor Content of the W+Jets Sample* CDF Note **8765** 2007

[11] J. Freeman, W. Ketchum, S. Poprocki, S. Pronko, V. Rusu, and P. Wittich *Search for Diboson Production in MET+$b\bar{b}$ channel* CDF Note **10204** [arXiv:1108:2060].

[12] F. Canelli et al. *Jet Energy Resolution* CDF Note **7856**

[13] H. L. Lai et al. *Global QCD Analysis of Parton Structure of the Nucleon: CTEQ5 Parton Distributions* Eur. Phys. J. C **12** (2000) 375 [arXiv:hep-ph/9903282v3].

[14] Tom Junk *Sensitivity, Exclusion and Discovery with Small Signals, Large Backgrounds, and Large Systematics* CDF Note **8128**

[15] F. James and M. Roos *MINUIT: A system For Function Minimization And Analysis Of The Parameter Errors and Correlations* Comput. Phys. Commun. **10** (1975) 343

[16] T. Aaltonen et al. (CDF Collaboration) *Measurement of the WW + WZ Production Cross Section Using the Lepton + Jets Final State at CDF II* Phys. Rev. Lett. **104** (2010) 101801.

[17] T. Aaltonen et al. (CDF Collaboration) *Invariant Mass Distribution of Jet Pairs Produced in Association with a W Boson in $p\bar{p}$ Collisions at $\sqrt{s}$ = 1.96 TeV* Phys. Rev. Lett. **106** (2011) 171801.

[18] W. Ketchum, V. Rusu, Y.K. Kim *Search for WZ/ZZ Production in leptons+jets channel* CDF Note **10581** (2011)

[19] G. Bellettini, G. Latino,V. Rusu, M. Trovato, G. Velev, C. Vernieri *Search for WZ/ZZ production in events with lepton(s) plus jets plus missing transverse energy* CDF Note **10630** (2011)

[20] R. Culbertson *et al.*, *Search for Anomalous Production of di-photon+MET Events in 2/fb of Data.*, CDF NOTE 9184

Appendices

A Investigating Matching to hadrons

The M_{RJC} distribution obtained in the sample in which jets are matched to either quarks and gluons (∼56%) shows a very good agreement between the two different methods of matching. The M_{RJC} distribution built in the whole sample in which the algorithm of matching to hadrons doesn't fail is shown in Fig. 19, left. It is compared to the same distribution obtained in the fully matched sample with the jets to partons association. The first distribution, built using hadron information, accepted more events than the second and the most part of them are in the low mass region. So it results a low mass tail in the M_{RJC} distribution we will use in our studies.
In Fig. 19, right, we show separately the comparison for each RJC.

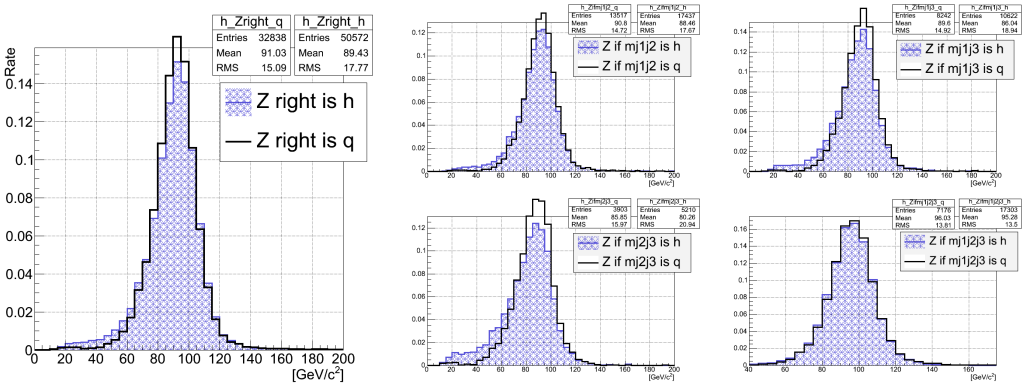

Figure 19: Left, We compare the M_{RJC} distributions, built in the sample in which jet are matched to hadrons (∼99% of the sample), with the one built using matching to partons information (∼56%). Right, the same comparison as done before, but separately for each RJC contribution.

We investigate the events in the low mass region and they are compatible with very high boosted events, see Fig. 20. When the decaying Z has a large boost, $q\bar{q}$ system is unbalanced and so the jet from the lowest E_T quark can be lost.
In the training of our NNs, the p_T information of the reconstructed bosons will be used in order to use the boost system information.

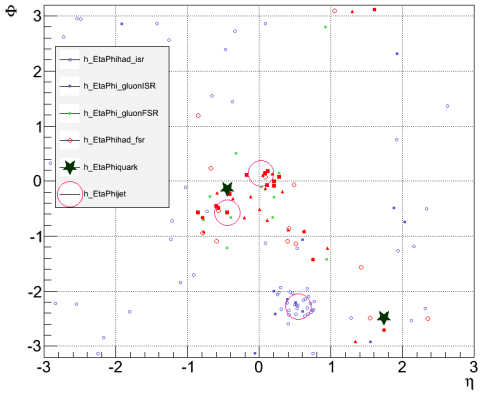

Figure 20: $\eta-\phi$ distribution of stable hadrons which comes from ISR and FSR, quarks and jets. The two quarks have respectively $E_T = 8$ and 76 GeV. The jet which should be associated to the less energetic quark is not reconstructed.

B NNs input in notag sample

B.1 Exploring MJ1J3: NN_{13}

As described before for NN_{12}, in order to isolate events when RJC = J1J3 we analyze differences of some variables in two subsamples, which now are defined as:

- RJC = J1J3
- Other jet combinations (RJC = J1J2, J2J3, J1J2J3, UNKNOWN) which we name "OJC"

Below is the list of the variables used (see Fig. 22):

1. $m_{jj'}/m_{j_1j_2j_3}$ [15]
2. $\gamma_{jj'} = (E_j + E_{j'})/m_{jj'}$
3. $\mathrm{d}\eta_{j_1j_2}$, $\mathrm{d}\eta_{j_2j_3}$
4. $dR_{j_1j_2}$, $dR_{j_2j_3}$
5. $\eta(j_1 + j_3)/\eta(j_2)$
6. $dR_{j_1j_2,j_3}$, $dR_{j_2j_3,j_1}$
7. $dR_{j_1j_2j_3,j_2}$
8. $dR_{j_2,\ell}$
9. Quark Gluon Discriminator for J3, J1
10. Ht
11. $Z_{p_T,13}$ related to the jet system 13.

Even in this case we decorrelate the NN_{13} output from the numerical value of MJ1J3 and make it sensitive only to the kinematical distributions of the involved variables (see Fig. 21).

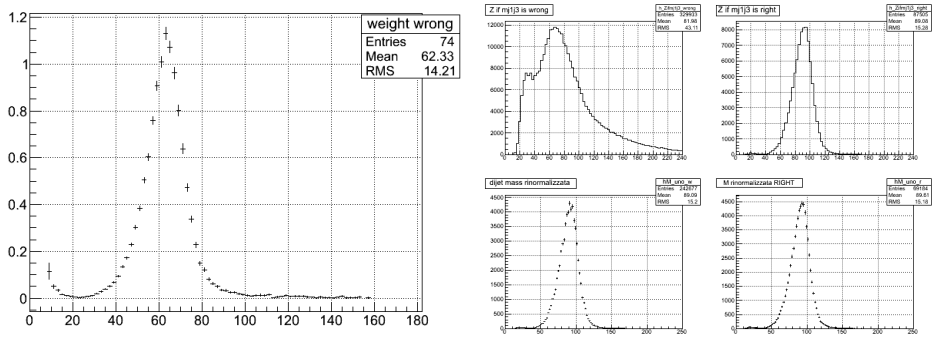

Figure 21: MJ1J3 distribution in the two subsamples before and after normalization (Right). Weights used for normalizing (Left).

B.1.1 Output

The NN_{13} response is shown in Fig. 23.

[15] jj' refers to the three possible combinations: J1J2, J1J3 and J2J3.

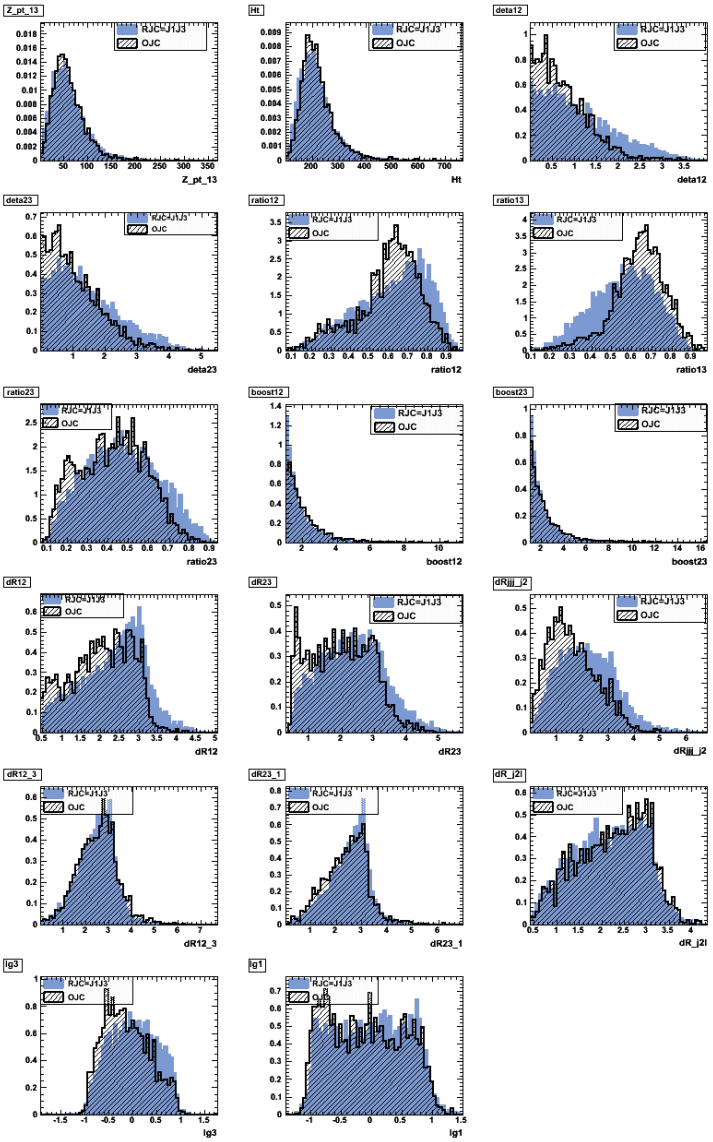

Figure 22: NN_{13} input variables after weighting.

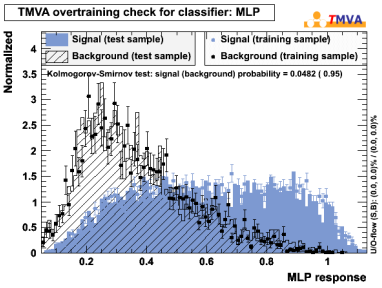

Figure 23: NN_{13} MLP response

B.2 Exploring MJ2J3: NN_{23}

In this case the two subsamples are defined as:

- RJC = J2J3
- Other jet combinations (RJC = J1J2, J1J3, J1J2J3, UNKNOWN) which we name "OJC"

Input variables in this case are, see also Fig. 25:

1. $m_{jj'}/m_{j_1j_2j_3}$[16]
2. $\gamma_{jj'} = (E_j + E_{j'})/m_{jj'}$
3. $\mathrm{d}\eta_{j_1j_2}$, $\mathrm{d}\eta_{j_1j_3}$
4. $p_T(j_2 + j_3)/p_T(j_1)$
5. $dR_{j_1j_2}$, $dR_{j_1j_3}$
6. $dR_{j_1j_2,j_3}$, $dR_{j_1j_3,j_2}$
7. $dR_{j_1j_2j_3,j_1}$
8. $dR_{j_2,\ell}$, $dR_{j_3,\ell}$
9. Ht
10. $Z_{p_T,23}$ related to the jet system 23.
11. Quark Gluon Discriminator for J2, J3

Even in this case we decorrelate the NN_{23} output from the numerical value of MJ2J3 in order to make it sensitive only to the kinematical distributions of the involved variables (see Fig. 24).

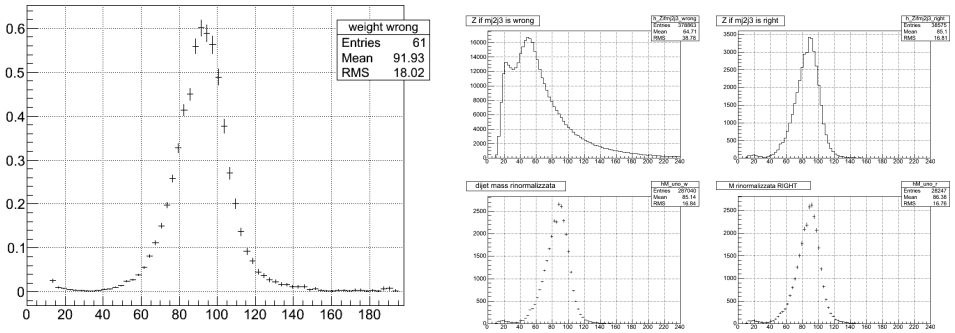

Figure 24: MJ2J3 distribution in the two subsamples before and after normalization (Right). Weights used for normalizing (Left).

B.2.1 Output

The NN_{23} response is shown in Fig. 26.

[16] jj' refers to the three possible combinations: J1J2, J1J3 and J2J3.

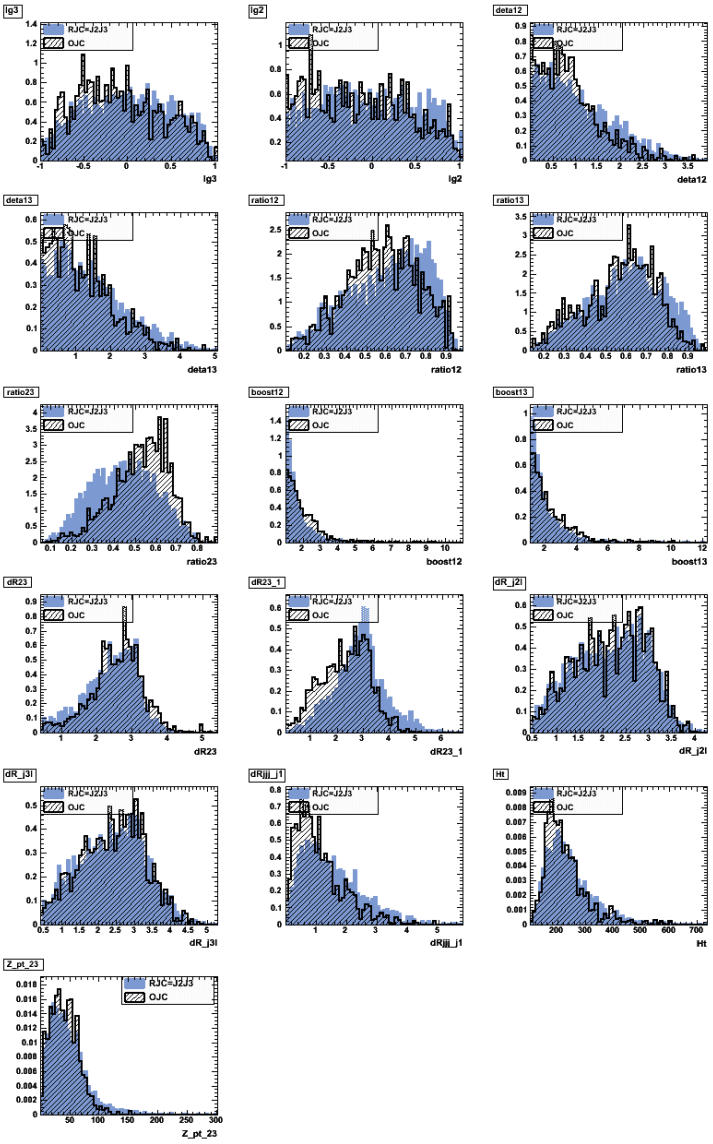

Figure 25: NN_{23} input variables after weighting.

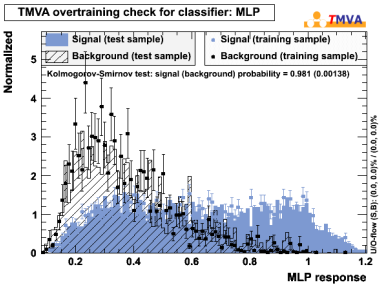

Figure 26: NN_{23} MLP response

B.3 Exploring MJ1J2J3: NN_{123}

NN_{123} aims at isolating the events in which FSR has occurred and for which Z-mass should be reconstructed using all the three jets. The subsamples we studied in this case are defined as:

- RJC = J1J2J3
- Other jet combinations (RJC = J1J2, J1J3, J2J3, UNKNOWN) which we name "OJC"

The input variables are (Fig. 28):

1. $\gamma_{jj'} = (E_j + E_{j'})/m_{jj'}$ [17]
2. $\gamma = (E_{j_1} + E_{j_2} + E_{j_3})/MJ1J2J3$
3. "pt-imbalance" : $p_{T\,j_1} + p_{T\,j_2} + p_{T\,j_3} - p_{T\,\ell}$−MET
4. $\mathrm{d}\eta_{j_1 j_3}$, $\mathrm{d}\eta_{j_2 j_3}$
5. $dR_{j_1 j_3}$, $dR_{j_2 j_3}$
6. $dR_{j_1 j_3, j_2}$, $dR_{j_2 j_3, j_1}$
7. $dR_{j_1 j_2 j_3, j_3}$
8. $dR_{j_3 \ell}$
9. Z_{p_t}
10. Quark Gluon Discriminator for J2, J3

In Fig. 27 are shown the weights applied to MJ1J2J3 distribution, calculated with the same criteria described for the other NNs. In Fig. 29 is shown the NN_{123} output.

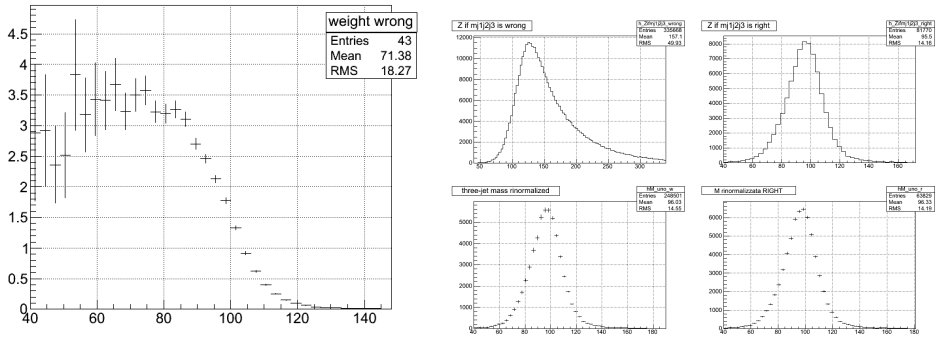

Figure 27: MJ1J2J3 distribution in the two subsamples before and after normalization (Right). Weights used for normalizing (Left).

B.3.1 Output

[17] jj' refers to the three possible combinations: J1J2, J1J3 and J2J3.

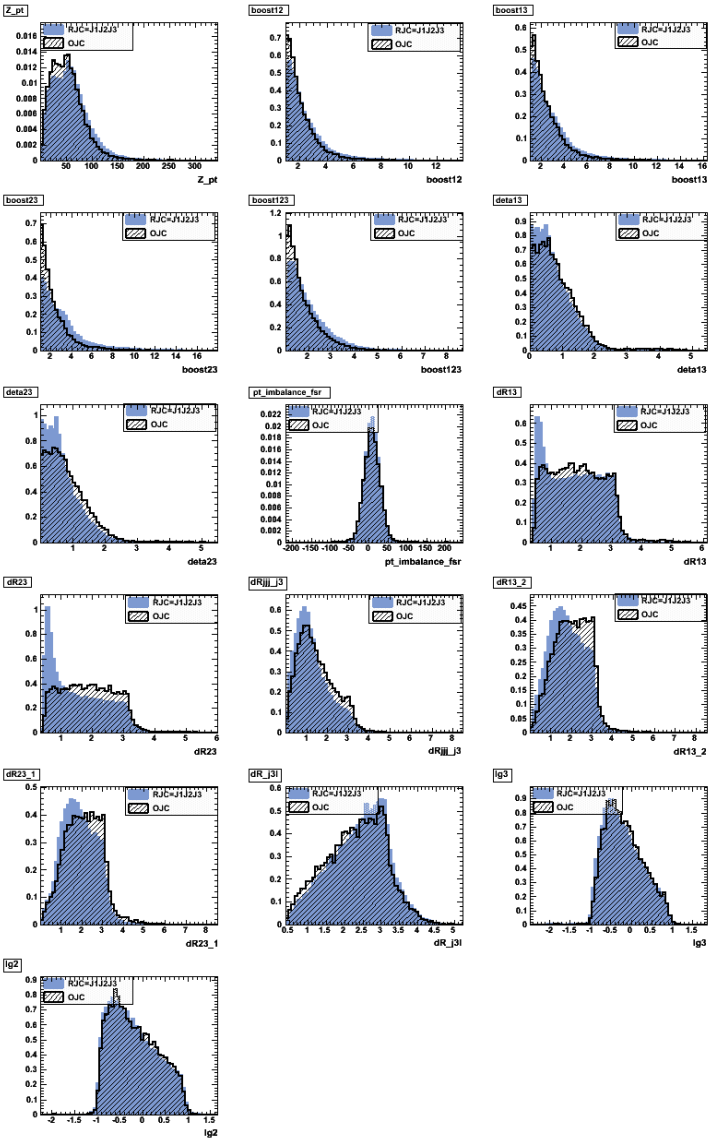

Figure 28: NN_{123} input variables after weighting.

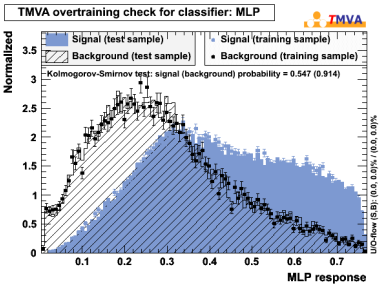

Figure 29: NN_{123} MLP response

C NNs input in tag sample

C.1 Exploring MJ1J2: NN_{12}

C.1.1 Input

Below is the list of the variables used:

1. $m_{jj'}/m_{j_1j_2j_3}$[18]
2. $\gamma_{jj'} = (E_j + E_{j'})/m_{jj'}$
3. $\mathrm{d}\eta_{j_1j_3}$, $\mathrm{d}\eta_{j_2j_3}$
4. $\eta(j_1 + j_2)/\eta(j_3)$
5. $dR_{j_1j_3}$, $dR_{j_2j_3}$
6. $dR_{j_1j_2,j_3}$, $dR_{j_2j_3,j_1}$
7. $dR_{j_1j_2j_3,j_3}$
8. $dR_{j_3,\ell}$
9. $b$ness for J1, J2
10. Quark Gluon Discriminator for J3

C.1.2 Output

The variables described above are weighted accordingly and are used for training a Neural Network, employing MLP method.
The NN_{12} response is shown in Fig. 31.

C.2 Exploring MJ1J3: NN_{13}

C.2.1 Input

Below is the list of the variables used:

1. $m_{jj'}/m_{j_1j_2j_3}$
2. $\gamma_{jj'} = (E_j + E_{j'})/m_{jj'}$
3. $\mathrm{d}\eta_{j_1j_2}$, $\mathrm{d}\eta_{j_2j_3}$
4. $dR_{j_1j_2}$, $dR_{j_2j_3}$
5. "pt-imbalance" : $p_{T\,j_1} + p_{T\,j_3} - p_{T\,\ell}-$MET
6. EMfr for J2 which is the ratio between EM and total energy.
7. $dR_{j_1j_2,j_3}$, $dR_{j_2j_3,j_1}$
8. $dR_{j_1j_2j_3,j_2}$, $dR_{j_1j_2j_3,j_3}$
9. $dR_{j_2,\ell}$, $dR_{j_3,\ell}$
10. Quark Gluon Discriminator for J2
11. $b$ness for J2

C.2.2 Output

Even in this case we decorrelate the NN_{13} output from the numerical value of MJ1J3 and make it sensitive only to the kinematical distributions of the involved variables. The NN_{13} response is shown in Fig. 33.

[18] jj' refers to the three possible combinations: J1J2, J1J3 and J2J3.

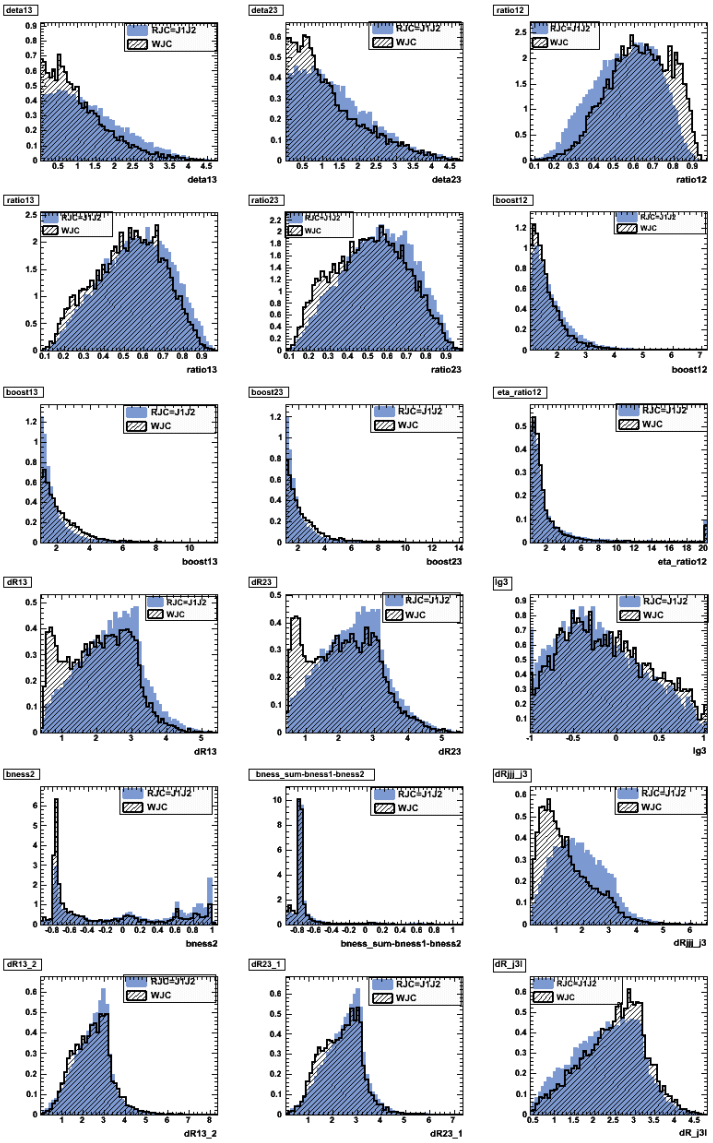

Figure 30: NN_{12} input variables after weighting.

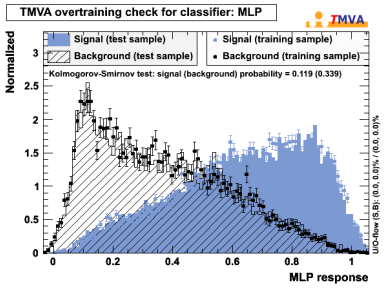

Figure 31: NN_{12} MLP response

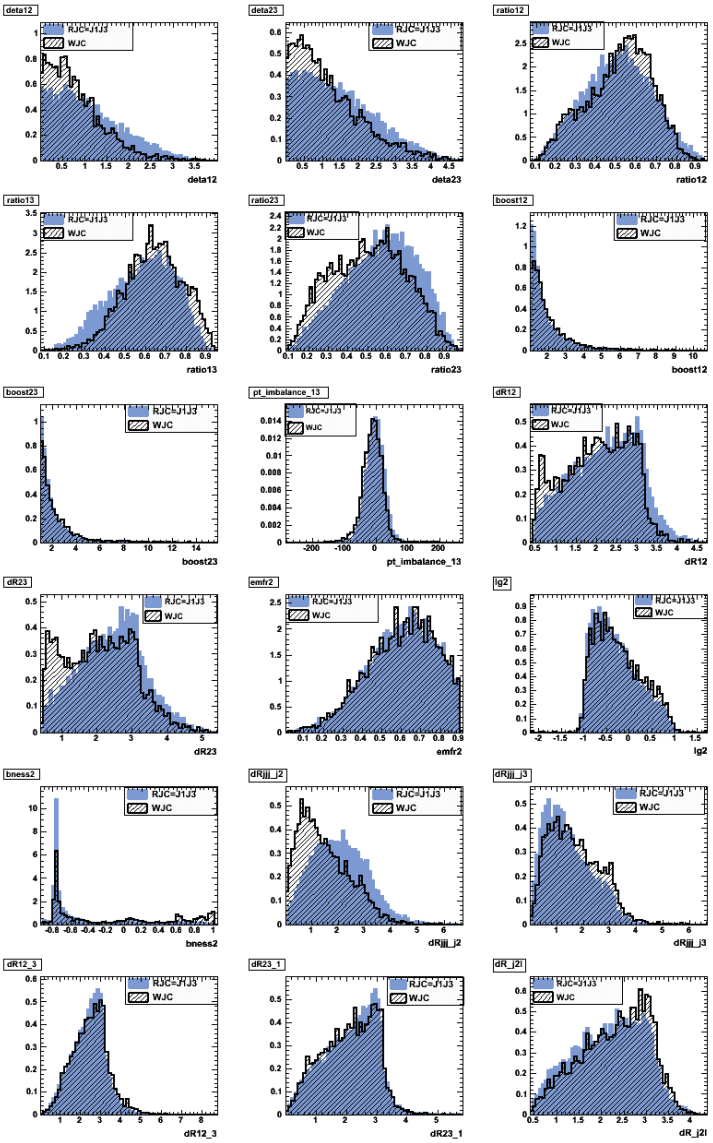

Figure 32: NN_{13} input variables after weighting.

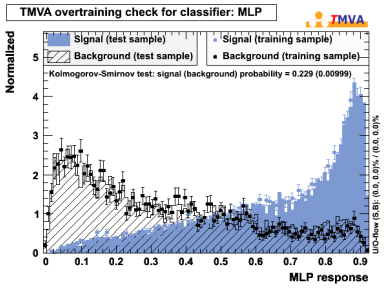

Figure 33: NN_{13} MLP response

C.3 Exploring MJ2J3: NN_{23}

C.3.1 Input

Input variables in this case are:

1. $\gamma_{jj'} = (E_j + E_{j'})/m_{jj'}$
2. $\mathrm{d}\eta_{j_1 j_2}$, $\mathrm{d}\eta_{j_1 j_3}$
3. $p_T(j_2 + j_3)/p_T(j_1)$
4. "pt-imbalance" : $p_{T\,j_2} + p_{T\,j_3} - p_{T\,\ell}-\mathrm{MET}$
5. $dR_{j_1 j_2}$, $dR_{j_1 j_3}$
6. $dR_{j_1 j_2, j_3}$, $dR_{j_1 j_3, j_2}$
7. $dR_{j_1 j_2 j_3, j_1}$
8. $dR_{j_1, \ell}$
9. $b$ness for J1, J3
10. Quark Gluon Discriminator for J1, J3

C.3.2 Output

Even in this case we decorrelate the NN_{23} output from the numerical value of MJ2J3 and make it sensitive only to the kinematical distributions of the involved variables.The NN_{23} response is shown in Fig. 35.

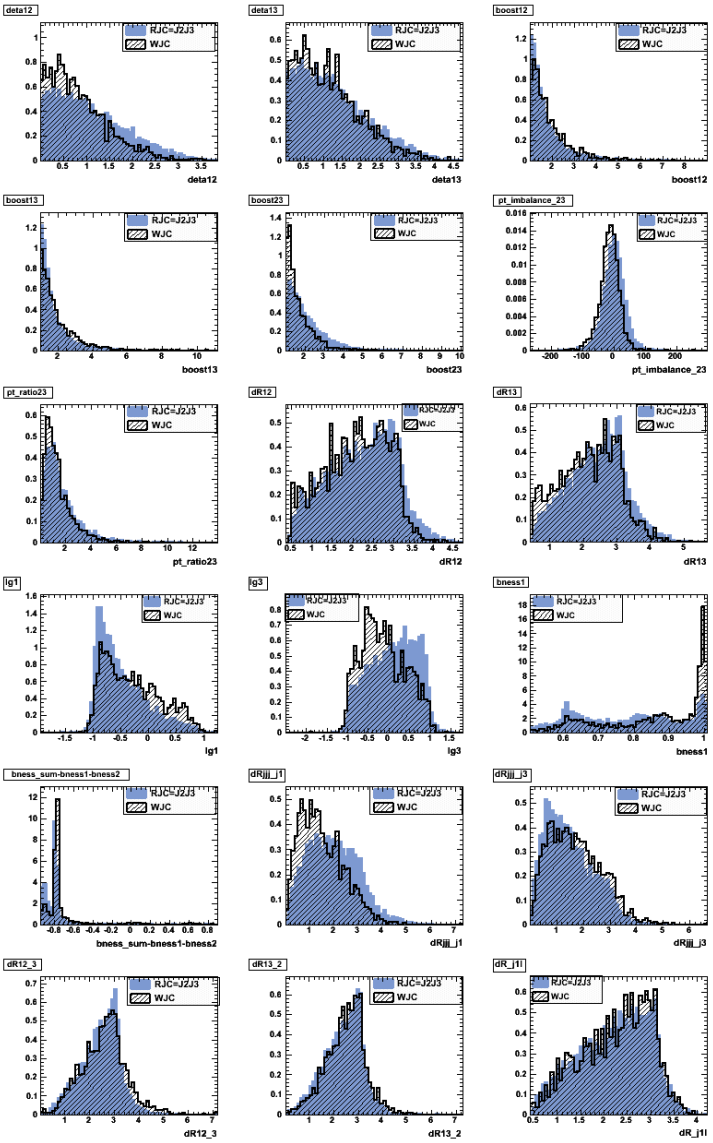

Figure 34: NN_{23} input variables after weighting.

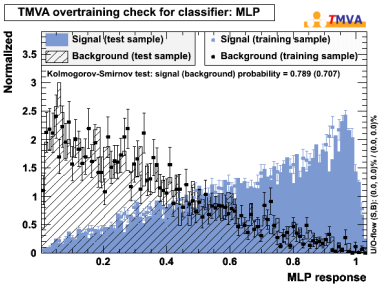

Figure 35: NN_{23} MLP response

C.4 Exploring MJ1J2J3: NN_{123}

C.4.1 Input

The input variables are:

1. $\gamma_{jj'} = (E_j + E_{j'})/m_{jj'}$ [19]
2. $\gamma = (E_{j_1} + E_{j_2} + E_{j_3})/MJ1J2J3$
3. "pt-imbalance" : $p_{T\,j_1} + p_{T\,j_2} + p_{T\,j_3} - p_{T\,\ell}$−MET
4. d$\eta_{jj'}$
5. $dR_{j_1 j_3}$, $dR_{j_2 j_3}$
6. $dR_{j_1 j_3, j_2}$, $dR_{j_2 j_3, j_1}$
7. $dR_{j_1 j_2 j_3, j_3}$, $dR_{j_1 j_2 j_3, j_2}$
8. $dR_{j_2 \ell}$, $dR_{j_3 \ell}$
9. EMfr for J2, J3
10. $b$ness J2, J3
11. Quark Gluon Discriminator for J2, J3

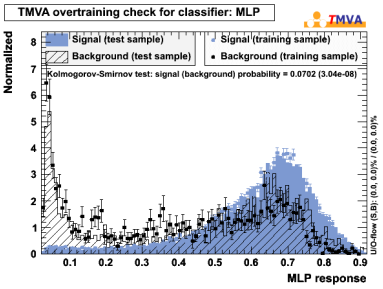

Figure 36: NN_{123} MLP response

C.4.2 Output

In Fig. 36 is shown the NN_{123} output.

[19] jj' refers to the three possible combinations: J1J2, J1J3 and J2J3.

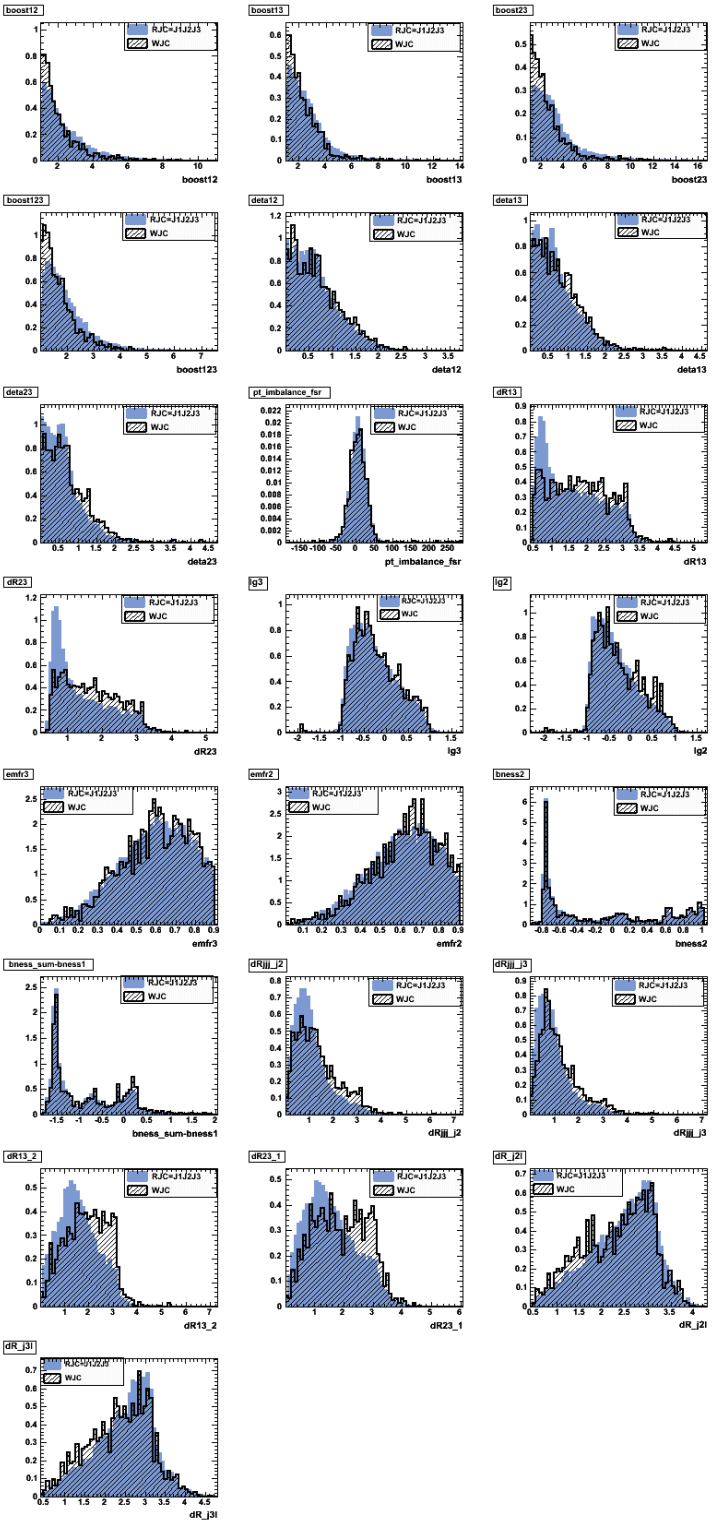

Figure 37: NN_{123} input variables after weighting.

D NNs Correlations

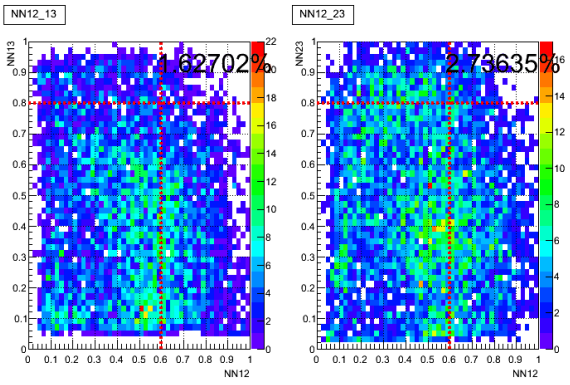

Figure 38:

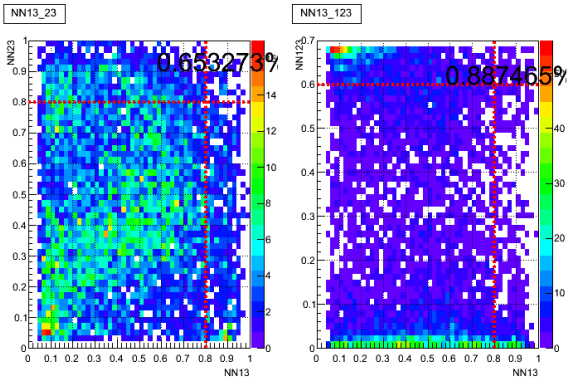

Figure 39:

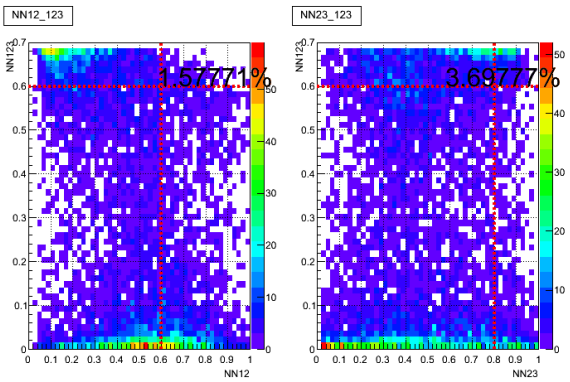

Figure 40:

E Resolution Parameters

E.1 Notag Sample

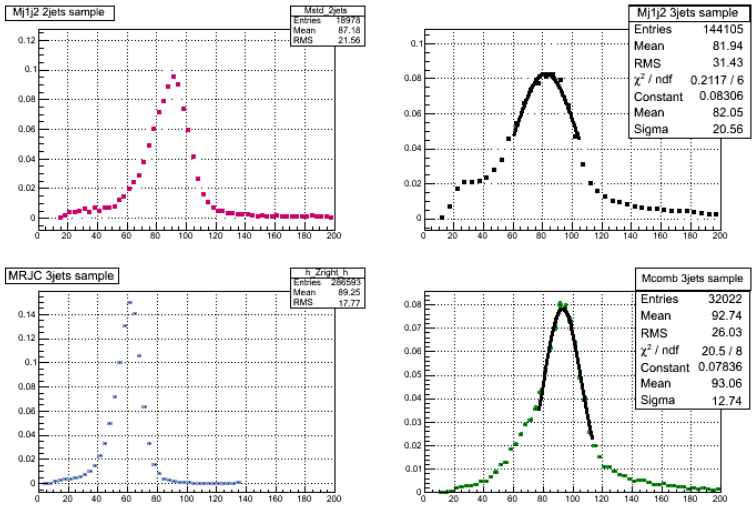

E.2 Tag Sample